Simulation of C-MEMS Based Enzymatic Biofuel Cell

Yamini S. Parikh, Varun Penmatsa, Jung-Hoon Yang, Chunlei Wang*
Mechanical and Materials Engineering Department, Florida International University
*Corresponding author: 10555 West Flagler Street, EC 3463, Miami, FL 33174, USA.
wangc@fiu.edu

Abstract: We optimize the performance of C-MEMS (Carbon-Micro Electro Mechanical system) based enzymatic biofuel cell (EBFC) by using finite elements analysis based COMSOL 3.4 Multiphysics software. With a simple model (one pair of electrodes) of BFC, we realized that most of the glucose is reacting with enzymes at the top of the posts and bottom of the posts remain deficient of the glucose. It is majorly due to slow diffusion of glucose in between high aspect ratio posts and high reaction rate of enzymes. We also could derive that the potential is highest when the height of posts is twice than that of well width. In a complex model (with multiple electrodes) of EBFC, potential distribution is shown by considering glucose and O_2 diffusion around posts and redox reaction of fuels based on enzyme kinetics. This complex design will lead us to find out the in depth relation between electrode posts geometry with that of output performance of EBFC.

Keywords: Enzymatic Biofuel Cell, Potential, Glucose.

1. Introduction

Biofuel Cell (BFC) is an electrochemical device which converts the chemical energy entrapped into biological fuel (in our case glucose) into electricity. They are used to power implantable electrically operated devices, such as pacemakers, defibrillators, insulin pumps, drug delivery systems. To facilitate the electron transfer between electrode surface and substrate, enzymes are immobilized onto both anode and cathode electrodes hence they are called EBFC. In our model, glucose oxidase (GOx) is immobilized onto anode and laccase is immobilized onto cathode. Despite the advantages such easy immobilization of enzymes on electrodes, sufficient selectivity for operation in membraneless format[1], improved longevity (up to 7-10days), current EBFCs cannot compete with conventional batteries because of their low cell voltages and power densities.

A biofuel cell power density is directly proportional to the electrode surface area as it provides more exposure to electrodes to react with substrate (glucose). As enzymes are immobilized onto electrodes, interaction of the substrate with electrode hence depends on the enzyme reaction rate and its concentration in polymer layer immobilized onto electrodes[2]. Ideally glucose should interact with the whole surface area of electrodes from top to bottom to fully utilize enzymes embedded onto it. Highly dense 3-D microarray structure has advantage of high surface area for reaction per footprint[1, 3], but same time response may not be improved if the electrode posts are not arranged wisely to provide sufficient space for glucose to diffuse in between the posts. Also due to high reaction rate of enzymes and improper selection of height of posts, most of the glucose will react immediately with the top portion of the electrode and the blood reacting with the bottom part of the electrodes remains deficient of glucose. So the selection of proper dimensions and geometry of the posts is also crucial to ameliorate the response of BFC[4]. So we are trying to provide and suggest the optimized design (relation between electrodes (of array) configuration (shape and dimensions) with respect to output potential and current response.) by using finite element analysis method which will help further establish experimental work.

2. Simple EBFC model

We have derived the relationship between geometry of electrode posts and output potential for one pair of electrode with very simple configurations. We are just using reaction rate according to different enzymes to consider enzymes immobilization on electrode posts. Any details regarding concentrations of enzyme values are not considered.

2.1 Mechanism/Theory of BFC

The redox mechanism of EBFC is shown below.

Overall Reaction:

$$\text{Glucose} + O_2 \xrightarrow{\text{GOx}} \text{Gluconolactone acid} + H_2O_2 \quad \text{-------1. 1}$$

Anode:

$$H_2O_2 \longrightarrow O_2 + 2H^+ + 2e^- \text{ (Oxidation)} \quad \text{-------1.2}$$

Cathode:

$$O_2 + 4H^+ + 4e^- \longrightarrow 2H_2O \text{ (Reduction)} \quad \text{------- 1.3}$$

Output potential is derived from the concentration of hydrogen ions, where hydrogen ions are considered to be linearly proportional to the glucose concentration around posts (As one mole of glucose will generate 2 moles of hydrogen ions).

The Nernst Planck's equations for output potential are shown below.

At anode:

$$E_{anode} = E^o_{anode} - (RxT/2xF) \ln ([H^+]^2 \text{ x } pO_2) \quad (V) \quad \text{------- 2}$$

At cathode:

$$E_{cathode} = E^o_{cathode} - (RxT/4xF) \ln([H^+]^{-4} \text{ x } pO_2) \quad (V) \quad \text{------- 3}$$

$$\text{Total cell voltage} = E_{anode} - E_{cathode} \quad (V) \quad \text{-------4}$$

2.2 Simulation

We have used convection and diffusion model along with conductive media DC module to show diffusion and potential response respectively. The steady state diffusion is considered for 50 s.

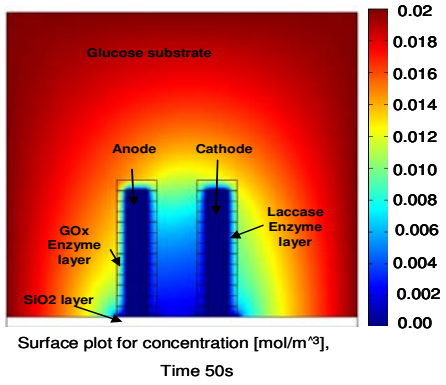

Figure 1: Surface plot of glucose concentration (mol/m^3) around electrode post: Height of posts 120um, Well width 60um, and Polymer thickness 10um.

Different reaction rate of GOx and laccase in the anode and cathode polymer layer are considered respectively. The diffusion and is shown in figure 1 above.

By plugging the Nernst Planck's equation at the boundary of enzyme layer-bulk interface we have derived potential response as shown in figure 2.

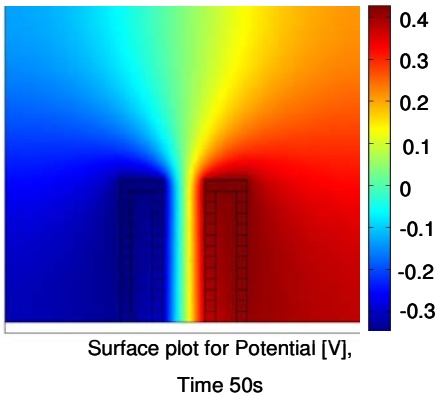

Figure 2: Surface plot of potential around posts. Boundary between bulk and enzyme layer is divided to provide varying potential boundary conditions to each sections.

From the plot we have measured the output potential difference from bottom of the posts. Parameters and constant values are shown in Appendix 1. We have assumed that there is no diffusion in the post which is valid as the posts are made up of solid carbon. Default module equations are being solved for this model.

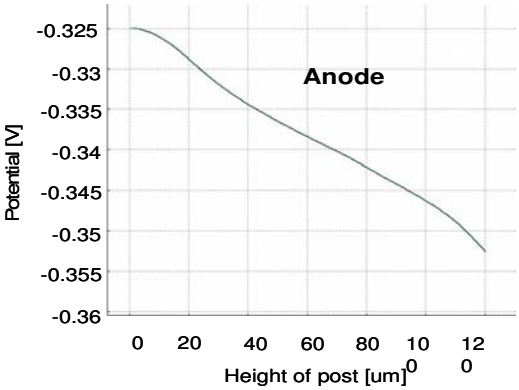

Figure 3: Potential curve vs. height of post at anode at 50 s.

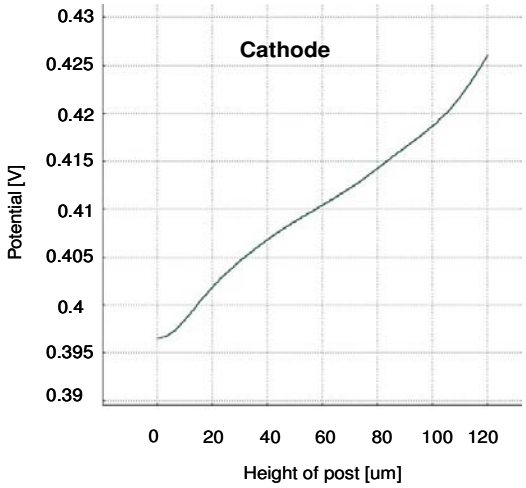

Figure 4: Potential curve vs. height of post at cathode at 50 s.

The same approach was used to simulate the output potential for different height of posts and well width (distance between two posts).

Also we could see from figure 1 that the diffusion of glucose at the bottom part of the posts is very much lesser than that at the top in between the posts, which shows the deficiency of glucose at the bottom part due to slow diffusion of substrate between high aspect ratio posts and high reaction rate in the enzyme layer. The reaction rate of GOx in anode layer was 4e-7[cm^2/s] and that in cathode layer was 7.6e-7[cm^2/s]. From figure 1 we can see that glucose is diffusing deeper till the bottom of anode than that at the cathode, which shows that less reaction rate gives deeper diffusion[5, 4]. Reason is that because of low reaction rate glucose will have chance to go to the bottom part before being reacted with enzymes. And hence we can have complete utilization of enzymes from top to bottom to generate potential. Potential generated in the post is again varying from top to bottom as the concentration is varying. Potential curves are shown in figures 3 and 4. From the simulations of different dimensions, we can surmise that the output potential is highest when the height of post is twice than that of well width. (Graphs are not shown here). This conclusion is in good agreement with our previous research results [1].

3. Complex EBFC model

This model is a more advanced model based on first model. In this model we have considered detailed enzyme kinetics and potential losses. This model will be further helpful to find out more accurate relation between output potential and geometry of posts. Here we have considered more than one pair of electrodes in the blood vessel. Theoretical model of enzyme kinetics and potential losses is explained in the section 3.1.

3.1 Theory

Enzyme Kinetics:

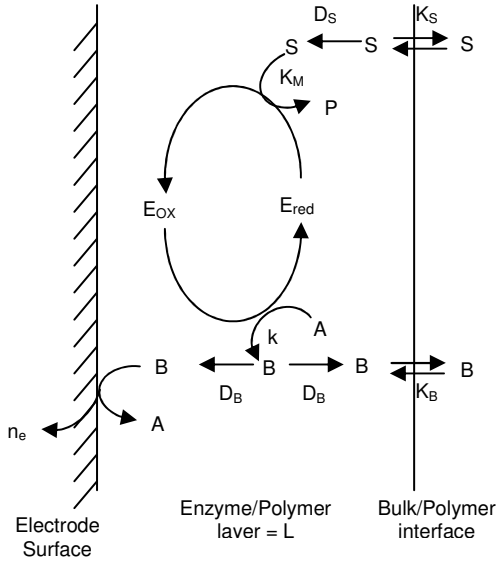

Figure 5: Schematic diagram of enzyme reaction in the polypyrrole film on the electrode.

- R = Gas constant 8.314472 J · K^{-1} · mol^{-1}
- T = 300K, Body temperature
- pO_2 = Partial pressure of oxygen in body
- e_0 = Concentration of total enzyme, (mmol/l)
- D_s = Diffusion coefficient of substrate into polymer film, (cm^2/s)
- e_{ox} = concentration of oxidized enzyme,(mmol/l)
- e_{red} = concentration of reduced enzyme,(mmol/l)
- k = charge transfer rate constant for oxidation of product (mmol/l/s)
- K_M = Michaelis-Menten constant (mmol/l)
- K_S = Partition coefficient of substrate in the film
- k_{cat} = catalytic reaction rate(s^{-1})
- L = film thickness (cm)
- A_k = distance to which substrate can diffuse in the film before being depleted by enzymatic reaction (cm)

Bartlett and Whitaker have described the general enzyme kinetics reaction in the polypyrrole film on the electrode which is shown in figure 5[2, 6, 7]. The enzyme catalyzed oxidation of substrate is assumed to follow the Michaelis-Menten kinetics[6] and the reduced form of the enzyme, E_{red} (GOD-$FADH_2$), is assumed to be regenerated by reaction with an oxidant O_2, to give the oxidized form of the enzyme, E_{ox} (GOD-FAD) and reduced oxidant, H_2O_2. Since over oxidized film is generally produced, H_2O_2 is thought to react only at the electrode surface. It is also assumed that glucose and H_2O_2 have partition coefficients, K_s and K_B, and diffusion coefficients in the film, D_s and D_B, respectively. Based on this reaction differential equations are derived for mass balance and transportation of substrate and products in the polymer film [2, 6, and 7]. Diffusion coefficient of substrate derived from that differential equation is used in the simulation which is as shown below.

$$D_s = \frac{A_k^{\,2} x K_{cat} x e_0}{K_M} \qquad \text{-------5}$$

Potential losses

For any BFC, When it is connected with an external resistance R_{ext} (also called ''load''), Ohm's law $V_{cell} = I*R_{ext}$ gives the fuel cell voltage, V_{cell}. Furthermore, the cell power is = $V_{cell}*I$. The actual fuel cell voltage is decreased from the equilibrium potential, E_{cell} (the maximum imposed by thermodynamics), by a series of irreversible losses $V_{cell} = E_{cell}$ - Losses. The equilibrium cell potential E_{cell} is expressed by the difference between the ideal equilibrium potentials of the cathode and anode, $EC^{(B)}$ and $EA^{(B)}$, respectively. The $EC^{(B)}$ and $EA^{(B)}$ at a moment in time are calculated as a function of the concentrations of reacting chemical species in the bulk liquid, S^B, at that moment. The losses, called overpotential or polarization, originate primarily from three sources: (1) activation overpotential (related to the rates of electrode reactions), (2) ohmic overpotential (related to the resistance to the flow of ions in the electrolyte and to flow of electrons through the electrode materials), and (3) concentration overpotential (related to mass transfer limitations of chemical species transported to or from the electrode[8, 9]. All these losses are also incorporated into the simulation.

Concentration potential equation:

$$E_{conc} = R*T * \ln (C_s/C_b) / (n*F) \qquad \text{-------6}$$

Activation potential equation:

$$E_{act} = R*T \ln (i / i_0) / (alpha*n*F) \qquad \text{-------7}$$

C_s = concentration of substrate at the bulk – polymer interface (assume that the diffusion is very small. Hence diffusion layer is taken from the electrode surface), C_b is the concentration in the bulk solution, T is the body temperature, alpha is the electro transfer coefficient of the reaction at the electrode, i_0 is the exchange current density.

3.2 Simulation

By using the diffusion coefficient and potential losses equation as shown above in equation 5, 6 and 7, we have derived the simulation response of diffusion of glucose and oxygen around anode and cathode and also from that potential distribution around posts. We have assumed that the glucose is only reacting with the anode polymer layer not with cathode layer and oxygen is only reacting with the cathode not with anode. Detailed parameters (Constants, subdomain expression and boundary expressions) used is shown in appendix 2.

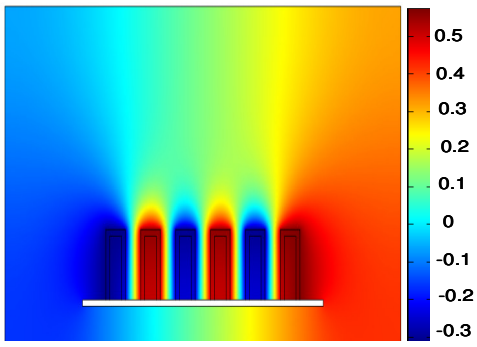

Figure 6: Surface plot of potential around electrodes. Steady state response time considered is 160 s. Height is 120um, well width is 40um, and polymer thickness is 10um. Posts are arranged as anode and cathode alternately from left. GOx layer on anode and Laccase layer is considered on cathode.

We can see from figure 6 that the potential losses is varying from top to bottom on the posts due to varying concentration of glucose interacting with the anode and varying concentration of oxygen interacting with the cathode. Graphs of potential for one pair of electrodes are shown in figures 7 and 8.

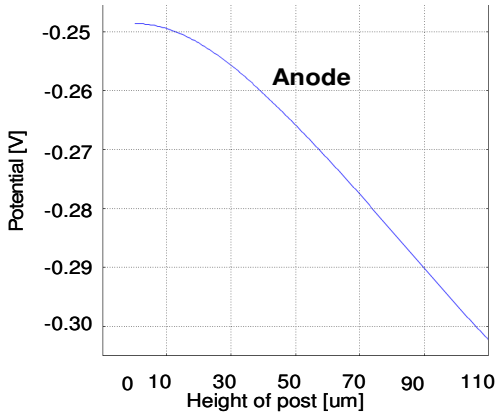

Figure 7: Potential in anode post (3rd post from left in fugre-6) vs. post height at 160 s.

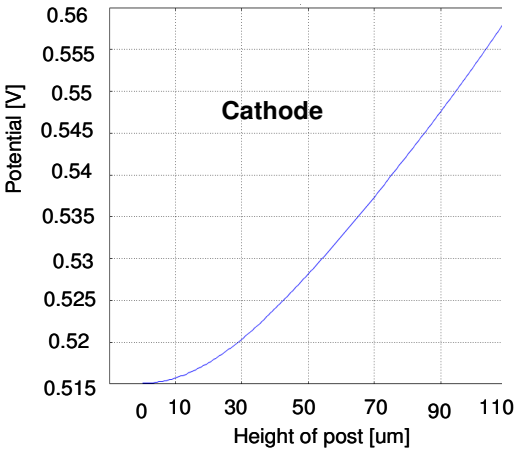

Figure 8: Potential in cathode post (4th post from left in fugre-6) vs. post height at 160 s..

From figures 7 and 8 we can say that the potential is varying from top to bottom due to varying concentration of substrate reacting with the posts. We will use this model to further find better geometry in terms of dimensions and shape, so that we can get uniform potential throughout the post and hence uniform current density which will help utilize the enzymes completely.

4. Conclusions

From our first simple module we have derived potential distribution and the relationship between electrode post height, well width and potential. Potential is highest when height of post is twice than that of well width. If we select ratio bigger than this then the transfer of electron from anode to cathode will not be efficient and if the ratio is lesser than this the concentration of glucose reaches to the bottom of the post will not be sufficient enough to generate more potential after reacting with enzymes.
From our complex model with all details we can see the potential response which shows all potential losses and also enzyme kinetics. It is yet to derive relationship between geometry (dimensions and shapes) of post and potential.

5. References

1. Michael J. Moehlenbrock, and Shelley D. Minteer, *Extended Lifetime Biofuel Cells.* Chemical Society Review, **37**: p. 1188-1196, (2008).
2. Min -Chol shin, Hyun C. Yoon, and Hak-Sung Kim, *Experimental and Theoritical Analyses on Factors Affecting the Performance of Polypyrrole/Glucose Oxidase Biosensor:Permeability Aspect of Polypyrrole Film.* Analytical Sciences,**12**, (1996).
3. Han Xu, Kartikeya Malladi, Chunlei Wang, Lawrence Kulinsky, Mingje Song, and Marc Madou, *Carbon Post-Microarrays for Glucose Sensors.* Biosensors and Bioelectronics, **23**: p. 1637–1644, (2008).
4. Venkataramani Anandan, Xiaoling Yang, Euihyeon Kim, Yeswanth Rao, and Guigen Zhang, *Role of Reaction Kinetics and Mass Transport in Glucose Sensing with Nanopillar Array Electrodes.* Journal of Biological Engineering, **1:5**, (2007).
5. Andrew kato Marcus, Cesar I. Torres, Bruce E. Rittmann, *Conduction-Based Modeling of the Biofilm Anode of a Microbial Fuel Cell.* Biotechnology & Bioengineering, **98**(6), (2007).
6. P. N. Bartlett, and R. G. Whitaker, *Electrochemical Immobilisation of Enzymes Part-I. Theory.* J. Electroanal. Chem., **224**: p. 27-35, (1987).

7. P. N. Bartlett, P. Tebbutt and R. G. Whitaker, *Kinetics Aspects of the Use of Modified Electrodes and Mediators in Bioelectrochemistry.* Prog. Reaction Kinetics, **16**: p. 55-155, (1991)
8. *Fuel Cell Handbook*. 7 ed.: ZPM Publishing, (2007).
9. Cristian Picioreanu, Ian M. Head, Krishna P. Katuri, Mark C. M. van Loosdrecht, and Keith Scott, *A Computational Model for Biofilm -Based Microbial Fuel Cells.* Water Research, **41**: p. 2921-2940.(2007).
10. P. Gros, A. Bergel and M. comtat, *Electrochemically Assisted Catalyst for Enzymatic Glucose Oxidation.* Chemical Engineering Science, **51**(10): p. 2337-2346, (1996).
11. E. E. Spaeth, and S. K. Friedlander, *The Diffusion of Oxygen, Carbon Dioxide and Inert Gas in Flowing Boold.* Biophysics Journal, **7**, (1967)
12. Noriaki Matsuda, and Kiyotaka Sakai, *Blood Flow and Oxygen Transfer Rate of an Outside Blood Flow Membrane Oxygenator.* Journal of membrane Science, **170**: p. 153-158, (2000)
13. J.L. Liu, D.A. Lowy, R.G. Baumann, and L.M. Tender, *Influence of Anode Pretreatment on Its Microbial Colonization.* Journal of Applied Microbiology, **102**(1): p. 177-183, (2007)
14. Frederic Barriere, Paul Kavanagh, and Donal Leech, *A Laccase-Glucose Oxidase Biofuel Cell Prototype Operating in a Physiological Buffer.* Electrochimica Acta, 2006. **51**: p. 5187-5192.

6. Acknowledgements

This project is funded by NSF NIRT grant (No. 0709085). Authors would like to thank Dr. Norman Munroe in Mechanical and Materials Engineering at Florida International University for helpful discussion.

7. Appendices

Appendix 1 Constants for simple model shown in section-2.

Constants name	Values (unit)	Description
R	8.314[J/(mol*K)]	Gas constant
T	300[K]	Body temperature_37° C
F	96485[C/mol]	Faraday's constant
RR	3.3e-6[mol/dm^3]	Reaction rate in the polymer layer at anode and cathode[3]
pO2	0.16[bar]	Partial pressure of oxygen inside body
Mul_c	1/(H2_ions_conc^4)* pO2	
Mul_a	(H2_ions_conc^2)*pO 2	
E_anode_ref	-0.32[V]	Ref. potential of anode according to GOx[14]
E_cathode_r ef	0.585[V]	Ref. potential of anode according to Laccase[14]
E_anode	E_anode_ref - ((0.5*R*T*log(Mul_a))/F)	Anode potential
E_cathode	E_cathode_ref + ((0.25*R*T*log (Mul_c))/F)	Cathode potential
Diff_laccase	7.6e-7[cm^2/s]	diffusion coefficient inside laccase layer
Diff_GOx	4e-7[cm^2/s]	diffusion coefficient inside glucose layer

Appendix 2: Constants for complex model shown in section 3.

Constants name	Values (unit)	Description
R	8.314[J/(mol*K)]	Gas constant
T	300[K]	Body temperature_37C
F	96485[C/mol]	Faraday's constant
Diff_glucose	6e-6[cm^2/s]	diffusion coefficient of glucose[3]
DsxKs	1.8e-9[cm^2/s]	Diffusion coefficient of substrate into film[2]
e0	L/Ak	Enzyme concentration[2]
Blood_den	1060[kg/m^2]	Blood density
Blood_visco	0.005[N*s/m^2]	Blood viscosity
Dapp	1.8e-9[cm^2/s]	Apparent diffusion coefficient
Ak	0.32[um]	Kinetic length[2]
Kcat	Dapp/(Ak^2)	Catalytic rate[2]
Ks	Dapp/Ds	Partition coefficient of substrate
Ds	((Ak^2)*Kcat*e0)/k_M	Glucose diffusion co efficient
Cb_g	25[mmol/l]	Bulk concentration of glucose[10]
n_a	2	Number of electron transfer at anode
Ht	0.42	Normal Hematocrit level in body (in percentage)
Diff_O2	(2.13-(0.0092*Ht))*(1e-9)[m2/s]	Diffusion co-efficient of oxygen[11, 12]
Vmax_a	3.3e-6[mol/dm^3]	Maximum reaction rate at anode
Vmax_c	3.3e-6[mol/dm^3]	Maximum reaction rate at cathode
Do	((Ak^2)*Kcat*e0)/Km	Oxygen diffusion inside laccase polymer layer
n_c	4	Number of electron transfer at cathode
Alpha	1000[1/s]	electron transfer constant
i0	6.1e-8[A/cm^2]	Exchange current density for glassy carbon[13]
Max_conc_g	100[mmol/l]	maximum glucose concentration[10]
Cb_o	0.24[mmol/l]	Oxygen concentration in bulk[10]
Max_conc_o	0.24*4[mmol/l]	Maximum Oxygen concentration[10]

Appendix 3 Subdomain/boundary expressions for model shown in section 3.

Subdomain/Boundary	Expression	Description
Anode enzyme layer	Vmax_a*(concentration of glucose)/(k_M+*(concentration of glucose))	Reaction rate in anode layer subdomain
Cathode enzyme layer	Vmax_c*(concentration of oxygen)/(k_M+*(concentration of oxygen))	Reaction rate in cathode layer subdomain
All anode boundaries	-0.32 - E_{conc} - E_{act}	Anode potential
All cathode boundaries	0.585 + E_{conc} + E_{act}	Cathode potential